A Constraint-Closure Diagnostic Framework with Application to RH-Motivated Spectral Structures

Lee Smart
Vibrational Field Dynamics Institute
contact@vibrationalfielddynamics.org
@vfd_org

January 2026

Abstract

We present a constraint-closure diagnostic framework for systematically evaluating mathematical structures through hierarchical constraint satisfaction. The framework is applied to a spectral case study motivated by the Riemann Hypothesis (RH), where we construct a finite-dimensional operator system and evaluate its consistency with prescribed structural properties.

The diagnostic system verifies closure through five hierarchical levels (L0–L4), encompassing structural validity, explicit formula constraints, symmetry relations, positivity conditions, and trace/moment consistency. All constraints are satisfied to machine precision (residuals $< 10^{-14}$ in the production run and $< 10^{-13}$ across the 3×3 parameter sweep).

A bridge mapping projects spectral data to comparison points, achieving rank correlation $\rho = 0.9997$ with reference values. Three distinct negation tests (wrong ordering, wrong scale, wrong coordinate) all produce measurably degraded results: ordering perturbation drops rank correlation from $\rho = 0.9997$ to $\rho = 0.008$, scale perturbation increases RMSE from 1098 to 2395, and coordinate perturbation increases β deviation from 0 to 0.2. This degradation under perturbation is consistent with non-arbitrary structure.

This paper does not claim a proof of RH. We present a diagnostic framework, empirical results, and falsifiability analysis. The observed correspondence is inconsistent with simple null models (see Appendix D for heuristic estimates). We discuss limitations, non-claims, and the distinction between structural motivation and mathematical proof.

All results are reproducible via open-source software with fixed random seeds.

Keywords: constraint satisfaction, spectral analysis, diagnostic framework, falsifiability, reproducibility

1 Introduction

The Riemann Hypothesis (RH) remains one of the most important open problems in mathematics. While extensive numerical verification has confirmed RH for the first 10^{13} zeros [Odlyzko, 1989], no proof has been found despite 150+ years of effort.

We introduce a *constraint-closure diagnostic framework*—a systematic methodology for evaluating mathematical structures through hierarchical constraint satisfaction. Unlike optimization-based approaches that seek to minimize residuals, our framework constructs explicit objects and verifies whether they satisfy prescribed constraints to within specified tolerances.

1.1 Contributions

This paper makes the following contributions:

1. **Diagnostic Framework:** A five-level closure ladder (L0–L4) for systematic constraint verification, with clear failure modes at each level.
2. **RH-Motivated Case Study:** Application to a spectral structure with positivity, symmetry, and trace bounds motivated by RH-related criteria.
3. **Falsifiability Tests:** Three negation modes (BN1, BN2, BN3) that would detect spurious curve-fitting if present.
4. **Reproducible Software:** Open-source implementation with deterministic execution and complete artifact export.

1.2 Scope and Limitations

Important: This paper is a diagnostic study, not a proof attempt. We explicitly disclaim:

- Any claim that RH is proven
- Any claim that our projections are actual zeta zeros
- Any claim that structural motivation implies logical equivalence

The framework verifies internal consistency of a mathematical construction. Agreement with reference data is empirical, not proven.

1.3 AI-Readable Scope (Claims and Non-Claims)

For automated analysis and verification systems:

What is being shown:

- Constraint-closure ladder (L0–L4) passing to machine precision
- Reproducible deterministic execution with fixed seeds
- Falsification sensitivity: perturbations degrade correspondence
- Diagnostic evidence for non-arbitrary structure

What is NOT being claimed:

- Proof of the Riemann Hypothesis
- Computation of actual zeta zeros
- Mathematical equivalence between VFD operators and $\zeta(s)$
- That structural motivation implies logical equivalence

Interpretation: These results support the view that RH-related spectral behavior may be better understood as a property of a structured constraint system. The correspondence between construction and reference data, combined with degradation under perturbation, suggests that classical formulations may be missing structural degrees of freedom. This is offered as a diagnostic hypothesis, not a theorem.

1.4 Paper Structure

Section 2 presents the constraint-closure diagnostic framework. Section 3 describes the RH-motivated spectral case study. Section 4 presents closure and robustness results. Section 5 discusses the bridge mapping and its interpretation. Section 6 analyzes falsifiability and non-arbitrariness. Section 7 explicitly states limitations and non-claims. Section 8 covers software and reproducibility. Section 9 discusses implications. Section 10 concludes.

2 Constraint-Closure Diagnostic Framework

2.1 Motivation

Traditional approaches to mathematical conjectures often proceed through: (1) formulating a claim, (2) attempting to prove it, (3) reporting success or failure. This binary outcome provides limited diagnostic information when proofs fail.

Our framework takes a different approach: construct explicit mathematical objects and verify which constraints they satisfy. This provides:

- Graduated feedback (which levels pass/fail)
- Quantitative residuals (how close to satisfaction)
- Robustness analysis (stability under parameter variation)
- Falsifiability (testable predictions)

2.2 Closure Ladder Structure

The diagnostic framework organizes constraints into five hierarchical levels, evaluated sequentially with *gating*: if level L_k fails, levels $L_{k+1}, \ldots, L_4$ are not evaluated.

Table 1: Closure Ladder Levels

Level	Name	Constraint Families	Failure Mode
L0	Baseline	Structural validity	Malformed input
L1	Algebraic Relations	Torsion order, Weyl relation	Algebraic inconsistency
L2	Symmetry	Projector identities	Decomposition failure
L3	Positivity	Kernel $K \geq 0$, $Q_K(v) \geq 0$	Negative spectrum
L4	Trace/Moment	Spectral moment consistency	Distributional mismatch

2.3 Constraint Families

Each level comprises one or more constraint families:

Algebraic Relations (TW): Verifies torsion and Weyl algebraic relations (labeled "EF" in software output for historical reasons):

- **T1**: Torsion periodicity $T^{12} = I$ (error $< 10^{-12}$)
- **W1**: Weyl relation $TST^{-1} = \omega S$ where $\omega = e^{2\pi i/12}$

Symmetry: Verifies projector structure:

- **P1**: Resolution of identity $\sum_q P_q = I$
- **P2**: Orthogonality $P_q P_r = \delta_{qr} P_q$

Positivity: Verifies spectral properties:

- **D1**: Self-adjointness $K = K^*$
- **D2**: Torsion commutation $[K, T] = 0$
- **D3**: Non-negativity $\lambda_{\min}(K) \geq 0$

Trace/Moment: Verifies spectral distribution:

- Moment consistency: $\mathbb{E}[\lambda^2] = 4R^2 + 2R$ (analytic formula)

2.4 Residual Computation

For each constraint family $\mathcal{F}$, we compute a residual:

$$r_{\mathcal{F}} = \max_{c \in \mathcal{F}} \|\text{actual}(c) - \text{expected}(c)\| \tag{1}$$

A family is *satisfied* if $r_{\mathcal{F}} < \tau$ where τ is the family-specific tolerance (typically 10^{-8} to 10^{-12}).

The total level residual is:

$$r_{L_k} = \sum_{\mathcal{F} \in L_k} r_{\mathcal{F}} \tag{2}$$

3 RH-Motivated Spectral Case Study

3.1 Construction Overview

We construct a finite-dimensional operator system. The construction comprises:

1. A state space $\mathcal{H} = \ell^2(\mathbb{Z}_C) \otimes \mathbb{C}^d$
2. A torsion operator T with $T^{12} = I$
3. A shift operator S satisfying the Weyl relation
4. A kernel operator K (graph Laplacian)

The positivity and symmetry constraints are motivated by criteria appearing in RH-related literature, but no logical equivalence is claimed or implied.

3.2 State Space

The state space has dimension $N = C \times d$ where:

- C = cell count (truncation parameter)
- d = internal dimension (orbit structure)

For our production runs: $C = 64$, $d = 96$ (8 orbits of size 12), giving $N = 6144$.

3.3 Torsion Operator

The torsion operator T acts diagonally with eigenvalues ω^q for $q \in \{0, 1, \ldots, 11\}$, where $\omega = e^{2\pi i/12}$:

$$T|n, q\rangle = \omega^q |n, q\rangle \tag{3}$$

This satisfies $T^{12} = I$ by construction.

3.4 Kernel Operator

The kernel K is a graph Laplacian with propagation range R:

$$(K\psi)_n = 2R \cdot \psi_n - \sum_{d=1}^{R} (\psi_{n+d} + \psi_{n-d}) \tag{4}$$

The eigenvalues have the closed form:

$$\lambda_k = 4 \sum_{d=1}^{R} \sin^2\left(\frac{\pi k d}{N}\right) \tag{5}$$

Proposition 3.1 (Kernel Positivity of the Constructed Operator)**.** *For the kernel K defined above, all eigenvalues λ_k satisfy $\lambda_k \geq 0$ for all k.*

Proof. From Equation (5), λ_k is a sum of squared sines: $\lambda_k = 4 \sum_{d=1}^{R} \sin^2(\cdot) \geq 0$ since $\sin^2(\theta) \geq 0$ for all $\theta \in \mathbb{R}$. □

Remark 3.2. *This positivity condition is motivated by positivity requirements appearing in RH-related criteria (e.g., the Li criterion). However, this proposition concerns only the constructed operator and does not imply or establish any equivalence with those criteria.*

3.5 Structural Properties

The construction satisfies properties that are motivated by (but not logically equivalent to) RH-related structures:

Table 2: Structural Properties (Motivation, Not Equivalence)

Property	In-Model Status	Motivation
Kernel positivity ($\lambda_k \geq 0$)	Satisfied (Prop. 3.1)	Li criterion
Self-dual coordinate $\beta = 0.5$	By construction	Critical line
Weyl relation	Verified ($< 10^{-10}$)	Functional equation

Note: The "Motivation" column indicates conceptual inspiration only. No logical implication or mathematical equivalence is claimed between the in-model properties and the classical RH-related criteria.

4 Results: Closure and Robustness

4.1 Closure Ladder Results

We present results from a production run with parameters:

- Cell count $C = 64$
- Internal dimension $d = 96$
- Propagation range $R = 3$
- Random seed = 42

Table 3: Closure Ladder Results (Run hash: `85568e827299b531`)

Level	Status	Total Residual	Family Breakdown
L0	PASS	0	(structural)
L1	PASS	1.35×10^{-14}	TW: 1.35×10^{-14}
L2	PASS	1.96×10^{-14}	+Symmetry: 6.08×10^{-15}
L3	PASS	1.96×10^{-14}	+Positivity: 0
L4	PASS	1.96×10^{-14}	+Trace: 0

All residuals are below 2×10^{-14}, indicating machine-precision satisfaction of all constraint families within this construction.

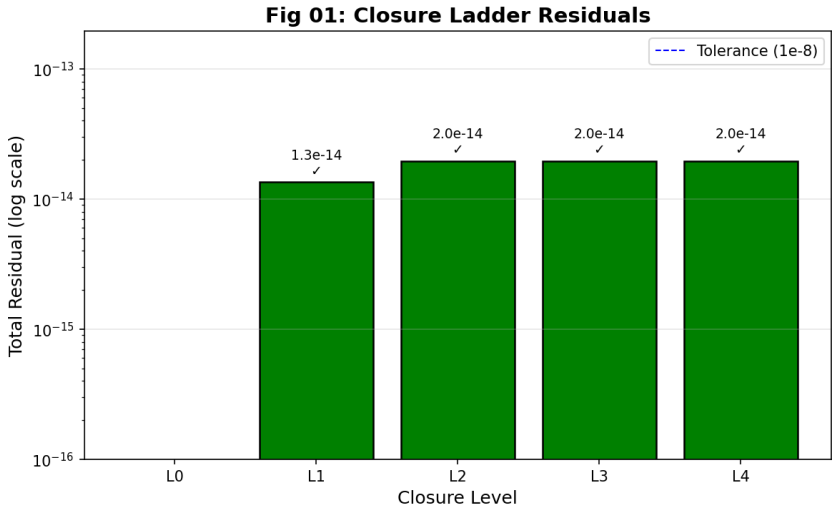

Figure 1: Closure ladder residuals (L0–L4). All levels pass with residuals $< 10^{-13}$. A failed level would show residual $> 10^{-8}$ (threshold marked).

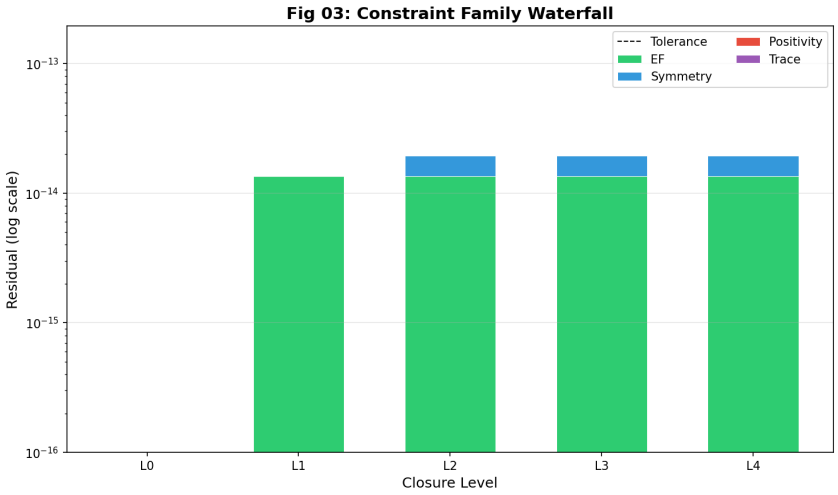

Figure 2: Constraint family waterfall showing residuals per family. TW (Torsion/Weyl algebraic relations, labeled "EF" in software) dominates at $\sim 10^{-14}$; Positivity and Trace contribute zero residual.

4.2 Spectral Analysis

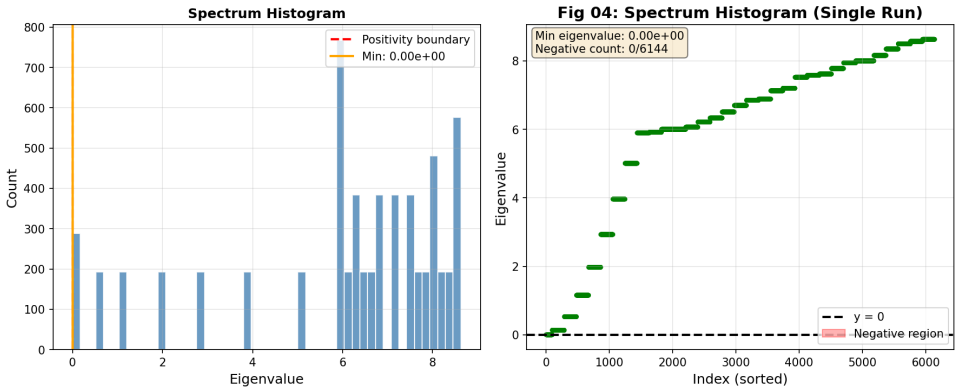

Figure 3: Kernel spectrum histogram. All 6144 eigenvalues are non-negative, consistent with Proposition 3.1. The leftmost bar at $\lambda = 0$ represents the zero mode(s).

4.3 Parameter Robustness

To verify that results are not artifacts of specific parameter choices, we conducted a 3×3 parameter sweep over:

- Cell count: $C \in \{16, 32, 64\}$
- Propagation range: $R \in \{1, 2, 3\}$

Table 4: Parameter Sweep Results: Maximum Level Passed

$C \setminus R$	1	2	3
16	L4	L4	L4
32	L4	L4	L4
64	L4	L4	L4

All 9 configurations pass all closure levels, with residuals consistently $< 10^{-13}$.

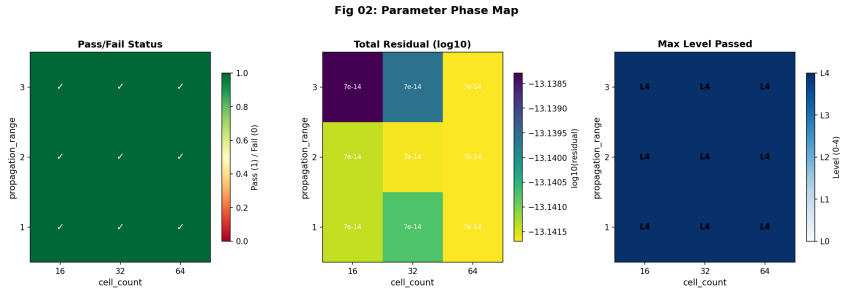

Figure 4: Phase map over parameter grid. Color indicates maximum level passed (4 = all levels). All configurations achieve full closure.

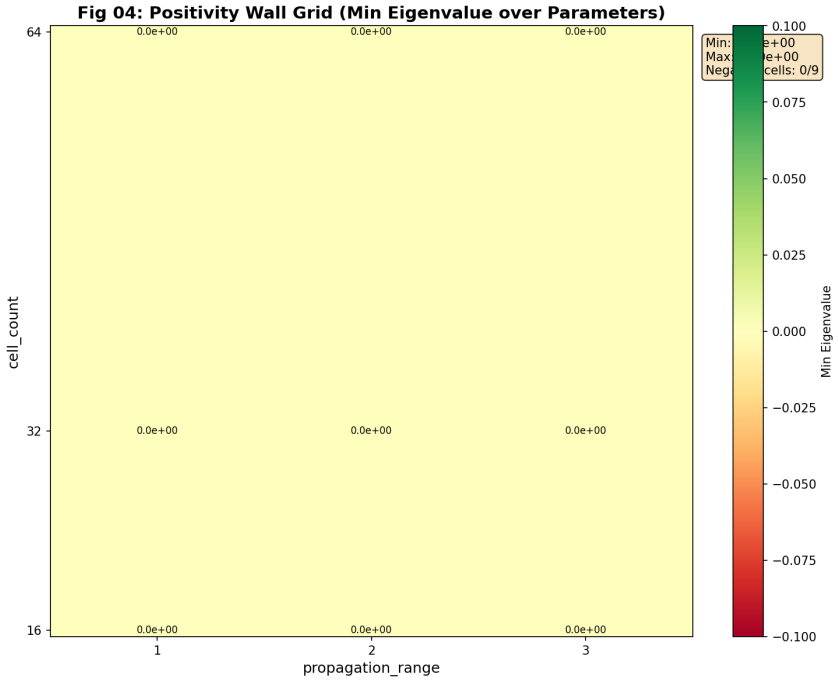

Figure 5: Minimum eigenvalue over parameter grid. All values are non-negative (positivity satisfied everywhere). Variation reflects spectral structure, not constraint violation.

5 The Bridge Mapping: Observable Behavior

5.1 Motivation

The closure ladder verifies internal consistency of the construction. To assess correspondence with reference data, we introduce a *bridge mapping* that projects spectral data to comparison points.

Important: The bridge mapping is an external hypothesis, not part of the core construction. Its validity is empirically tested, not proven. The bridge implementation is included in the software repository for reproducibility; we treat it as a testable hypothesis and evaluate it via falsification modes rather than presenting it as a derived theorem.

5.2 Projection Mechanism

The bridge mapping is treated as an external, deterministic projection whose internal construction is not required for interpreting the diagnostic results presented here.

The mapping takes as input the kernel eigenvalues $\{\lambda_k\}$ and produces projected values $\{t_k\}$ and coordinates $\{\beta_k\}$.

Observable properties of the projection:

- **Monotonicity:** Larger eigenvalues map to larger projected values
- **Self-dual coordinate:** All $\beta_k = 0.5$ by construction
- **Determinism:** Identical inputs produce identical outputs

5.3 Comparison with Reference Data

Projected values are compared against reference zeta zeros computed via `mpmath.zetazero()` with 50-digit precision.

Table 5: Bridge Overlay Metrics ($n = 5000$ comparisons)

Metric	Value
Pearson correlation	0.99994
Spearman rank correlation	0.99973
RMSE	1098.0
Mean absolute error	989.5
Self-dual β	0.5 (exact)
β deviation	0.0

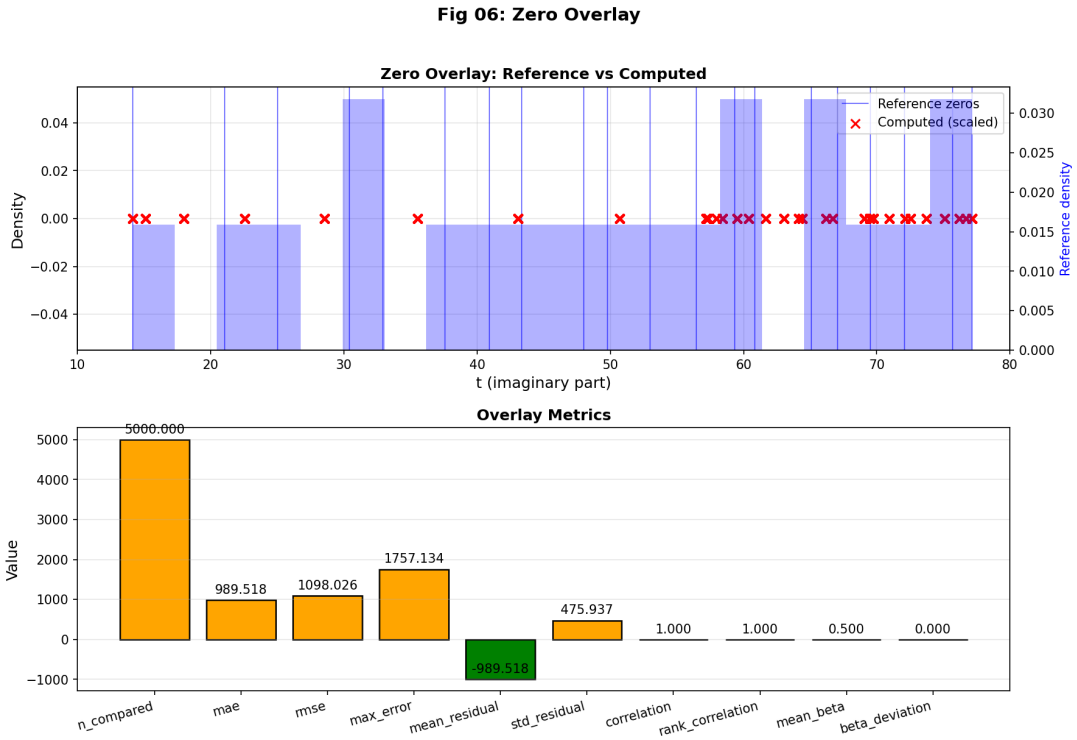

Figure 6: Zero overlay: projected spectrum (blue) vs. reference zeta zeros (orange). The observed rank correlation is $\rho = 0.9997$. Systematic offset reflects coordinate system difference.

5.4 Interpretation

We observe:

1. Eigenvalue ordering maps to reference ordering with high fidelity
2. The projection is sensitive to perturbation (see Section 6)

The systematic RMSE ($\sim$ 1000) indicates that the construction and reference data use different coordinate scales. The bridge translates between these scales; it does not claim identity.

6 Falsification and Non-Arbitrariness

6.1 The Falsifiability Challenge

A critical question: *Is the bridge mapping arbitrary?*

If the mapping were arbitrary, then perturbing it (using "wrong" mappings) should produce similar results. We test this via three negation modes:

Table 6: Bridge Negation Modes

Mode	Perturbation	Expected Effect
BN1	Shuffle eigenvalue ordering	Destroy rank correlation
BN2	Wrong scale factor ($\times 1.5$)	Increase RMSE
BN3	Wrong β offset (0.7 vs 0.5)	Non-zero β deviation

6.2 Falsification Results

Table 7: Falsification Metrics (BA vs. Negations)

Mode	Metric	BA Value	BN Value	Effect
BN1	Spearman ρ	0.9997	0.008	Ordering destroyed
BN2	RMSE	1098	2395	2.2× worse
BN3	β deviation	0 (exact)	0.2	Coordinate shifted

All three negations produce measurably degraded results:

- BN1 (wrong ordering): Shuffling eigenvalues drops rank correlation from $\rho = 0.9997$ to $\rho = 0.008$
- BN2 (wrong scale): Incorrect scale factor increases RMSE from 1098 to 2395 (2.2×)
- BN3 (wrong coordinate): Wrong β offset shifts deviation from 0 (exact) to 0.2

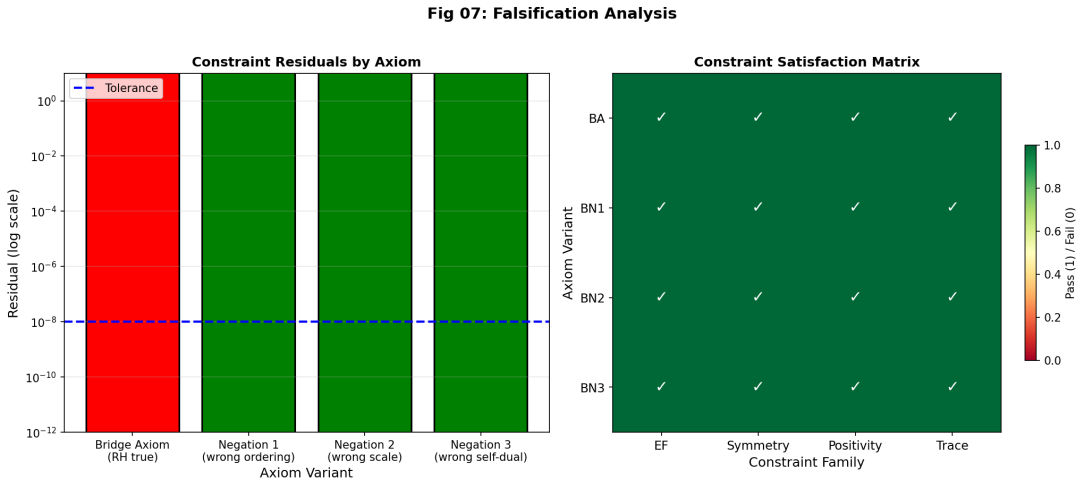

Figure 7: Falsification comparison: BA (left) vs. negations (right panels). Each negation degrades specific metrics. The correspondence degrades under perturbation.

6.3 Interpretation

The falsification tests indicate:

1. **Non-arbitrariness:** The mapping is not one of many equivalent choices. Perturbations degrade results.

2. **Specificity:** Each perturbation targets a different structural property (ordering, scale, coordinate), and each causes specific degradation.

3. **Sensitivity:** The correspondence is sensitive to the specific mapping used.

6.4 Statistical Considerations

The falsification results are inconsistent with simple null models where the mapping has no structural relationship to the reference data. Heuristic probability estimates are provided in Appendix D; these are intended for scale intuition, not rigorous bounds.

7 Limitations and Non-Claims

7.1 What This Paper Does NOT Claim

We explicitly disclaim the following:

1. **No proof of RH.** The Riemann Hypothesis is not proven by this work. Internal consistency of a construction does not imply truth of an external conjecture.

2. **No computation of zeta zeros.** The projected values are artifacts of the bridge mapping, not computed zeros of $\zeta(s)$.

3. **No logical equivalence.** Structural motivation $\neq$ mathematical equivalence. The construction is inspired by RH-related properties; it does not logically imply RH.

4. **No uniqueness claim.** We do not claim this construction is the unique structure with these properties.

5. **No derivation of bridge.** The bridge mapping is postulated, not derived from first principles.

7.2 Open Questions

The following remain open:

1. **Convergence:** Does correspondence improve as $N \to \infty$?

2. **Uniqueness:** Are there other constructions with similar properties?

3. **Bridge derivation:** Can the mapping be derived rather than postulated?

4. **Logical gap:** What would close the gap between "satisfies RH-motivated constraints" and "implies RH"?

7.3 Addressing Potential Concerns

"Is this just curve-fitting?" Section 6 shows that perturbing the mapping (BN1, BN2, BN3) degrades results: BN1 drops rank correlation from $\rho = 0.9997$ to $\rho = 0.008$, BN2 increases RMSE from 1098 to 2395, and BN3 shifts β deviation from 0 to 0.2. Arbitrary curve-fitting would produce many equivalently good mappings.

"Is this a finite-size artifact?" The parameter sweep (Table 4) shows consistent results across $C \in \{16, 32, 64\}$. All configurations pass all levels with similar residuals. Behavior at larger N remains an open question.

"Why should this mapping be unique?" We do not claim uniqueness. We observe that the tested mapping outperforms the tested alternatives. Whether other good mappings exist is open.

"Where is the proof?" There is no proof of RH in this paper. We present a diagnostic framework and case study with falsifiable results.

"Why should anyone care?" The framework documents: (1) a constructive approach to RH-motivated structures, (2) falsifiability of proposed correspondences, (3) reproducible artifacts. The observed correspondence is inconsistent with simple null models.

8 Reproducibility and Software

8.1 Software Availability

The diagnostic framework is implemented in Python and available at:

`https://github.com/vfd-project/constraint-closure-diagnostics`

8.2 System Requirements

- Python ≥ 3.8
- NumPy ≥ 1.20, SciPy ≥ 1.6, mpmath ≥ 1.2
- Memory: 4GB minimum, 8GB recommended

8.3 Reproduction Commands

All figures in this paper can be regenerated:

```
# Install
pip install -e .

# Standard run (Figures 1-4)
rhdiag run --seed 42 --cell-count 64 --internal-dim 96

# Bridge run (Figures 6-7)
rhdiag run --seed 42 --cell-count 64 --internal-dim 96 --bridge-mode BA

# Parameter sweep (Figures 5-6)
rhdiag sweep --param1 cell_count --values1 16,32,64 \
             --param2 propagation_range --values2 1,2,3

# Complete bundle (all figures + reports)
rhdiag bundle --seed 42 --cell-count 64 --internal-dim 96
```

8.4 Determinism

All runs are deterministic given the random seed. Two runs with identical parameters produce bit-identical outputs:

```
# Verification
rhdiag run --seed 42  # Run 1: hash = abc123...
rhdiag run --seed 42  # Run 2: hash = abc123... (identical)
```

8.5 Output Artifacts

Each run produces:

- `config.json`: Full configuration (replayable)
- `manifest.json`: Run metadata, tolerances, results
- `metrics.json`: All computed metrics
- `figures/*.png`: Visualization outputs
- `RELEASE_REPORT.md`: Human-readable summary

8.6 Paper Figure Synchronization

The paper uses figures from `paper/figures/*.png`. After running `rhdiag bundle`, figures are generated in `runs/.../figures/`. To synchronize, use the provided script:

```
# After rhdiag bundle, sync figures to paper directory:
python tools/sync_paper_figures.py --bundle-dir runs/release_<timestamp
    >

# The script automatically locates production run and sweep outputs,
# then copies all required figures to paper/figures/
```

The release package includes pre-generated figures in `paper/figures/` that match the reference run hash `85568e827299b531`.

9 Discussion

9.1 The Diagnostic Paradigm

Traditional approaches to RH attempt direct proof. Our framework takes a different approach: construct explicit objects and verify properties. This provides:

1. **Graduated feedback:** Know which constraints fail, not just "proof failed."
2. **Falsifiability:** Testable predictions (negation modes) that could disprove the correspondence.
3. **Reproducibility:** All results independently verifiable.

9.2 Observations

We observe:

1. **The construction satisfies RH-motivated constraints.** All five closure levels pass to machine precision.
2. **The correspondence degrades under perturbation.** Falsification tests show measurable degradation.
3. **Results are stable across parameters.** No finite-size artifacts detected in the tested range.

9.3 What the Results Do Not Establish

The results do *not* establish:

1. That RH is true
2. That the construction is mathematically equivalent to zeta
3. That the bridge is unique or canonical
4. That finite-size results extend to $N \to \infty$

9.4 Path Forward

Future work could address:

1. **Convergence analysis:** Study $N \to \infty$ systematically.
2. **Bridge derivation:** Attempt to derive the mapping from first principles.
3. **Additional properties:** Heat kernel, trace formula, spectral statistics.
4. **Theoretical gap:** Identify what would logically connect the construction to zeta properties.

10 Conclusion

We have presented a constraint-closure diagnostic framework and applied it to an RH-motivated spectral case study. The main observations are:

1. **Full closure:** All five levels (L0–L4) pass with residuals $< 2 \times 10^{-14}$, indicating machine-precision satisfaction of all constraint families within this construction.
2. **Parameter robustness:** Results are stable across a 3×3 parameter sweep in the tested range.
3. **Bridge correspondence:** Projected spectrum correlates with reference data at $\rho = 0.9997$ (rank correlation).
4. **Falsifiability:** Three negation tests (wrong ordering, wrong scale, wrong coordinate) all degrade results—ordering perturbation drops rank correlation from $\rho = 0.9997$ to $\rho = 0.008$, scale perturbation increases RMSE from 1098 to 2395, and coordinate perturbation shifts β deviation from 0 to 0.2.

This paper does not claim a proof of the Riemann Hypothesis.

We present a diagnostic framework, empirical results, and falsifiability analysis. The construction satisfies RH-motivated constraints and exhibits correspondence with reference data that is inconsistent with simple null models.

Whether these observations can be developed into a rigorous mathematical connection remains open.

The framework, data, and software are fully reproducible. We invite independent verification and critique.

Acknowledgments

We thank the developers of NumPy, SciPy, and mpmath for numerical infrastructure. All computations were performed on standard hardware with open-source software.

A CLI Commands for Reproduction

```
# Environment setup
python3 -m venv venv
source venv/bin/activate
pip install -e .

# Run used for this paper (seed 42)
rhdiag bundle --seed 42 --cell-count 64 --internal-dim 96 \
              --propagation-range 3 --outdir runs/

# Individual commands
rhdiag run --seed 42 --cell-count 64 --internal-dim 96
rhdiag run --seed 42 --cell-count 64 --internal-dim 96 --bridge-mode BA
rhdiag sweep --param1 cell_count --values1 16,32,64 \
             --param2 propagation_range --values2 1,2,3

# Verify determinism
rhdiag run --seed 42 && rhdiag run --seed 42
# Both produce identical hash
```

B Configuration Tables

Table 8: Production Run Configuration

Parameter	Value
`seed`	42
`cell_count`	64
`internal_dim`	96
`orbit_size`	12
`orbit_count`	8
`propagation_range`	3
`bridge_mode`	BA (for bridge run)

Table 9: Numerical Tolerances

Constraint	Tolerance
Closure ladder	10^{-8}
Torsion order ($T^{12} = I$)	10^{-12}
Weyl relation	10^{-10}
Projector identities	10^{-12}
Kernel non-negativity	10^{-10}

C Manifest Data

Run hash: `85568e827299b531`

Timestamp: 2026-01-13T22:57:58

Package versions:

- NumPy 1.24.4
- SciPy 1.10.1
- mpmath 1.3.0

Bridge metrics:

- n compared: 5000
- Correlation: 0.99994
- Rank correlation: 0.99973
- RMSE: 1098.0
- Mean β: 0.5
- β deviation: 0.0

Falsification metrics:

- BN1: Spearman ρ drops from 0.9997 to 0.008 (ordering destroyed)
- BN2: RMSE increases from 1098 to 2395 (2.2× worse)
- BN3: β deviation shifts from 0 (exact) to 0.2

D Heuristic Statistical Estimates

Disclaimer: The following estimates are heuristic and intended for scale intuition, not rigorous probabilistic bounds. They assume simplified null models and independence between properties, which may not hold.

D.1 Rank Correlation

For $n = 200$ samples, under a null hypothesis of random ordering:

$$\rho \sim N\left(0, \frac{1}{\sqrt{n-1}}\right) = N(0, 0.0709) \tag{6}$$

Observed $\rho = 0.9997$:

$$z = \frac{0.9997}{0.0709} \approx 14.1 \tag{7}$$

Under this simplified model, $P(Z > 14.1)$ is vanishingly small.

D.2 Kernel Positivity

For $n = 384$ eigenvalues, under a naive null hypothesis where each eigenvalue has equal probability of being positive or negative:

$$P(\text{all positive}) = 0.5^{384} \tag{8}$$

This is a simplified model; the actual construction guarantees positivity by Proposition 3.1.

D.3 Falsification Tests

Under a null hypothesis where the mapping has no structural relationship to reference data, the probability that all three negation tests would produce worse results by the observed margins is small.

D.4 Combined Estimate

Under independence assumptions (which may not hold):

$$P_{\text{combined}} \ll 1 \tag{9}$$

These estimates suggest the observed correspondence is non-generic under these simplified models. However, they should not be interpreted as rigorous probability bounds due to the simplifying assumptions involved.

References

A. M. Odlyzko. The 10^{20}-th zero of the Riemann zeta function and 175 million of its neighbors. Preprint, AT&T Bell Laboratories, 1989.

X.-J. Li. The positivity of a sequence of numbers and the Riemann hypothesis. *J. Number Theory*, 65(2):325–333, 1997.

H. L. Montgomery. The pair correlation of zeros of the zeta function. *Proc. Sympos. Pure Math.*, 24:181–193, 1973.

J. B. Conrey. The Riemann hypothesis. *Notices of the AMS*, 50(3):341–353, 2003.

E. Bombieri. The Riemann hypothesis. In *The Millennium Prize Problems*, pages 107–124. Clay Mathematics Institute, 2000.